Available online at www.sciencedirect.com
ScienceDirect
Journal of Catalysis 253 (2008) 148–158
JOURNAL OF CATALYSIS
www.elsevier.com/locate/jcat

Solvent effects in the epoxidation reaction of 1-hexene with titanium silicalite-1 catalyst

Chen E. Ramachandran [1], Hongwei Du, Yoo Joong Kim [2], Mayfair C. Kung, Randall Q. Snurr, Linda J. Broadbelt *

Institute for Catalysis in Energy Processes and Department of Chemical and Biological Engineering, Northwestern University, Evanston, IL 60208, USA

Received 12 July 2007; revised 10 October 2007; accepted 11 October 2007

Abstract

The epoxidation of 1-hexene with titanium silicalite-1 (TS-1) catalyst was investigated to gain insight into the effect of the solvent on the observed reactivity. Three different solvents were examined: methanol, acetonitrile, and acetone. Kinetic data were obtained from batch reaction experiments, with an emphasis placed on gathering more accurate initial rates than those reported in the literature. The dependencies of the rates on the concentrations of 1-hexene, water, and hydrogen peroxide were determined. The adsorption behavior of 1-hexene in TS-1 in the three different solvents was determined independently by batch sorption experiments. Results showed that the solvent has a significant effect on the adsorption of 1-hexene, and hence on the reaction kinetics. Kinetic modeling incorporating experimental and simulated quaternary adsorption isotherms to describe quasi-equilibrated steps revealed that the differences in the observed reaction kinetics may be attributed mostly, but not entirely, to differences of the partitioning of 1-hexene between the bulk and intraporous phases among the three different solvents.

Keywords: Solvent effects; Titanium silicalite-1; TS-1; 1-Hexene adsorption; 1-Hexene; Epoxidation; Silicalite; Multicomponent adsorption in silicalite

1. Introduction

The catalytic oxidation of olefins to epoxides (oxiranes) is of great importance to the chemical industry, because epoxides are valuable intermediates for a wide variety of bulk chemicals, polymers, and fine chemicals. In olefin epoxidation processes, the development of titanium molecular sieves has drawn considerable attention in the last two decades, with very promising catalysts with high activity and selectivity emerging. One such catalyst, titanium silicalite (TS-1), has proven to be highly selective in the liquid-phase oxidation of a wide range of hydrocarbons, including alkenes, alkanes, alcohols, and aromatics [1–8]. TS-1 has a zeolitic MFI framework comprising silicon, oxygen, and a small amount of isolated titanium atoms. Epoxidation reactions with TS-1 can be performed at ambient temperatures and pressures using hydrogen peroxide as the oxidant, thus forming only water as a byproduct. The unique properties of TS-1 with hydrogen peroxide as the oxidant have been attributed in part to the hydrophobicity of the mostly siliceous structure [9,10]. Recently, it has been shown that the hydrophobicity of TS-1 can be impacted by how it is synthesized, thereby affecting reaction rates and selectivities [11]. Furthermore, it has been determined that the titanium in TS-1 is less prone to leaching under reaction conditions compared with other titanium molecular sieves [12–15]. This is in contrast to silica-supported isolated titanium catalysts [16] or the Shell amorphous titania silica catalyst, which in addition is inactive with aqueous hydrogen peroxide due to the strong adsorption of water at the titanium site [5].

The oxidative properties of TS-1 arise from the intraporous, isolated, framework titanium atoms, which are believed to be tetrahedrally coordinated [17], possibly with a distorted tetrahedral form [18–20]. The siting of titanium atoms in TS-1 is still being debated [21–27]. Although no consensus exists regarding the siting of titanium, there is no evidence to date suggesting

* Corresponding author. Fax: +1 (847) 491 3728.
E-mail address: broadbelt@northwestern.edu (L.J. Broadbelt).
[1] Present address: Shell Global Solutions, Houston, TX, USA.
[2] Present address: ALZA Corporation, Mountain View, CA, USA.

0021-9517/$ – see front matter
doi:10.1016/j.jcat.2007.10.016

that titanium in different sites will result in differences in reactivity and selectivity, especially for substrates that are not sterically bulky.

Titanium also can exist in TS-1 in the form of anatase [28], but its formation in TS-1 is undesirable, because anatase comprises clusters of octahedrally coordinated titanium atoms, which can have different reactivity than the isolated tetrahedrally coordinated titanium of the framework [29]. Studies have suggested that extra-framework titanium species can cause the decomposition of hydrogen peroxide [30,31], as well as the formation of undesired side products, both with unknown kinetics. In addition, there is the concern of pore blockage by anatase [17]. Typically, the amount of extra-framework titania is not quantified in the literature, but its presence could greatly complicate the analysis of kinetic data, so anatase formation should be avoided.

In liquid-phase systems using TS-1 as the catalyst and hydrogen peroxide as the oxidant, solvents are used to prevent phase separation of the organic reactants and aqueous hydrogen peroxide. However, solvents also have been found to significantly affect the reactivity and selectivity of TS-1-catalyzed reactions [28,32–36], although the mechanisms for such solvent effects are not completely understood. Three hypotheses have been put forth for the origin of the solvent effects. First, it has been proposed that the solvent influences the intrinsic reaction kinetics at the active titanium site. Second, it has been theorized that the solvent affects adsorption behavior, thereby altering intraporous concentrations and concentrations at the active site of reactants and products. Finally, it has been suggested that intraporous diffusivities are affected by the solvent and that diffusion could affect the observed reaction rate.

The earliest hypothesis put forth was that the solvent imparted intrinsic differences in reactivity of the titanium site through coordination [32,37]. It was hypothesized that different solvents directly affect the intrinsic reactivity of the titanium sites based on their ability to coordinate with titanium; however, there is no spectroscopic evidence of such a species, and the exact nature of the active species is unclear [7,36,38,39]. Furthermore, because TS-1 systems are prone to deactivation [40], many studies have not captured true initial rates that are free of deactivation effects [41,42], thereby masking intrinsic kinetics. Although some correlations exist between reported reaction rates and the different properties of some solvents such as polarity, electrophilicity, or molecular size, no correlation captures the behavior of all solvent systems [43]. More recently, quantum chemical calculations by Sever and Root [44,45] found no effects of the solvent on the activation barrier or reaction rate of ethylene epoxidation. However, experimental and theoretical studies have converged on one aspect of the active site structure: that it is some form of a titanium hydroperoxo species [44,46–49].

Recently, the important role of the solvent in determining adsorption behavior in TS-1–catalyzed epoxidation of olefins was highlighted by Jacobs and coworkers [33,34]. The partition coefficient of adsorption, defined as the ratio of intraporous concentration to extraporous concentration, was determined for the reactant using a tracer chromatographic method. The partition coefficients in the Henry's law regime for 1-hexene in various solvents were ranked in the same order as reactivity, suggesting that adsorption plays an important role in the reaction. However, the tracer chromatographic method can only determine the partition coefficients in the Henry's law regime, where there is a linear dependence between the intraporous and bulk liquid concentrations. Because reactions typically encompass a wider range of reactant concentrations, a more extensive adsorption study is needed to establish and quantify the impact of solvents on this component of the overall reaction kinetics.

Finally, a limited number of studies have shown that the solvent can affect the diffusivity of species relevant to epoxidation in MFI. Ramachandran et al. [50] used PFG NMR to study the diffusivity of *n*-hexane in silicalite in methanol, acetonitrile and acetone solvent as a nonreacting mimic for 1-hexene in TS-1. The results demonstrated that epoxidation of 1-hexene is not diffusion-limited unless the crystal size of TS-1 is >38 μm.

To provide further insight into the role of solvent in olefin epoxidation, we have studied the adsorption and reaction of 1-hexene and hydrogen peroxide using TS-1 as the catalyst in three different solvents: methanol, acetone, and acetonitrile. Batch reaction experiments were carried out with an emphasis on obtaining initial rate data, and adsorption experiments were carried out over a wide range of concentrations. Finally, the experimental data were summarized in a serviceable kinetic model from which quantitative insights about the relative contributions of the effect of solvent on adsorption and reaction to the overall kinetics could be gained.

2. Experimental

2.1. TS-1 and silicalite synthesis and regeneration

TS-1 was synthesized hydrothermally using a modified procedure of Thangaraj et al. [51]. First, double-deionized water (DDI) was added to two-thirds of the tetrapropylammonium hydroxide (TPAOH, 40% aq, Alfa Aesar), and the mixture was stirred until uniform. Tetraethylorthosilicate (TEOS, 99+%, Aldrich) was then added dropwise to the TPAOH mixture and stirred until the solution became clear. Separately, titanium butoxide (TiBuOH, 99+%, Alfa Aesar) was mixed with dry isopropyl alcohol (IPA, 99.5%, Aldrich) and then added dropwise to the TEOS/TPAOH mixture under vigorous magnetic stirring. This was followed by the dropwise addition of the remaining TPAOH mixed with DDI. This final mother liquor was stirred for 1 h and then poured into a 200-ml Teflon-lined autoclave. The following molar proportions of each reagent were used: 1TEOS:0.36TPAOH:30DDI:2.1IPA:1.3TiBuOH.

Crystallization in the autoclaves took place in a 160 °C oven for three weeks in 200-ml autoclaves. At the end of the crystallization period, the catalyst was recovered by centrifugation and washed with DDI until a pH of 7 was reached.

The recovered catalyst was calcined in air in a muffle furnace. The temperature was ramped at a rate of 2 °C/min up to 110 °C, where it was maintained for 10 min, then ramped by 2 °C/min up to 530 °C and maintained there for 10 h before re-

turning to room temperature. After calcination, the catalyst was kept in a desiccator until use.

Regenerated catalyst also was used for the reaction and adsorption experiments. Regeneration involved calcining spent catalyst in air twice using the following profile: ramp of 1 °C/min up to 110 °C and maintenance there for 5 h, followed by a ramp of 0.5 °C/min up to 530 °C and maintenance there for 10 h before cooling to room temperature.

The silicalite samples used for the adsorption study were synthesized using the same procedure as for TS-1, except that no TiBuOH was added.

2.2. Characterization

To ensure that the synthesized TS-1 catalyst was free of extra-framework titanium species or impurities, the samples were subjected to multiple analytical techniques. In addition, regenerated catalyst was characterized to ensure that the regeneration was successful and that the catalyst sustained no damage to its structural integrity or to the state of the active titanium sites.

X-ray powder diffraction (XRD) analysis of TS-1 was carried out on a Sintag PAD V diffractometer to determine the crystallinity. Also, quantitative phase analysis was carried out using the General Structure Analysis System (GSAS) software program to determine the framework titanium content, based on the established correlation between unit cell volume and framework Ti content [1,30].

Inductively coupled plasma (ICP) analysis (using a Hitachi model 180-80) was performed to determine the total amount of titanium and impurities present in the TS-1 and silicalite samples. For the analysis, TS-1 and silicalite were dissolved using a mixture of HF and HCl in DDI. Individual SPEX CertiPrep standards (Fisher Scientific) were used as the reference calibration standards (i.e., Na, K, Ti, Fe, Al, and Si), using the same concentration of HF and HCl in the DDI matrix as in the TS-1 sample.

Diffuse-reflectance UV–vis analysis was carried out on a Cary 500 UV–vis spectrometer equipped with a Varian diffuse reflectance accessory comprising a 110-mm-diameter PTFE-coated integrating sphere, a high-performance photomultiplier tube, and a lead sulfide detector. Calibration was based on the 100% absorption black-colored slide and a 100% reflectance PTFE baseline reference disk (Labsphere).

X-ray photoelectron spectroscopy (XPS), using an Omicron ESCA Probe equipped with an electron flood gun and a scanning ion gun, was used to determine the surface composition of TS-1. Carbon was used as a reference for peak positions, and a separate titanium(IV) anatase sample was used to distinguish between anatase (458.8 eV) and framework titanium (460.4 eV) in the TS-1 sample. The anatase sample was also used to obtain the sensitivity factor for titanium. Sensitivity factors for silicon and oxygen were obtained from previous calibrations and were similar to published values [52].

Infrared spectroscopy (IR) was performed on a Bio-Rad FTS-40 FTIR to ascertain the existence of the 960-cm^{-1} peak. The TS-1 sample was pressed with KBr. The BET surface area was determined with a Micromeritics ASAP 2400 at liquid nitrogen temperature. The scanning electron microscopy (SEM) image of TS-1 was obtained using a Hitachi 4500 microscope.

2.3. Adsorption experimental setup

Omnifit NMR tubes (Wilmad Glass) were used for the experimental adsorption study. Catalyst preparation entailed pressing the catalyst into a pellet and then breaking the pellet into pieces small enough to fit through the 5-mm opening of the NMR tube. Addition of the catalyst and liquid into the NMR tubes was done in a such manner that the catalyst did not adhere to the glass above the liquid level. The tubes were then fitted with Omnifit valves containing PTFE/silicon septa (Wilmad Glass). A liquid mixture was prepared separately in a 4-ml vial, in which the deuterated solvent (Cambridge Isotopes: acetone-d_6, 99.9%; methanol-d_4, 99.8%; acetonitrile-d_3, 99.8%) was added, followed by addition of mesitylene (as the internal standard), 1-hexene, and DDI water. The liquid mixture was injected using gas-tight syringes into three NMR tubes, one tube containing no catalyst which was used as a control, one tube containing silicalite, and one tube containing TS-1. Valves were closed immediately to seal the sample and prevent evaporation of reagents. A control experiment without catalyst demonstrated little or no evaporation over a period of weeks. All Omnifit NMR systems were weighed after the addition of catalyst and the addition of the liquid. Prepared samples were allowed to equilibrate undisturbed for at least 48 h at room temperature (22–24 °C). At the end of the equilibration period, the concentration of the bulk liquid phase above the settled catalyst was determined using ^{1}H NMR.

The samples were analyzed on an Inova 500 NMR spectrometer equipped with VNMR analysis software. The Omnifit tubes were positioned in the NMR rotors so that only the liquid above the catalyst level was analyzed. T_1 relaxation times were determined for each solvent system and at least five times that quantity was used for the recycle delay. In each analysis, eight transients or scans were used, 6.0×10^4 points were taken for each scan, and 1.31×10^5 Fourier zeroes were added to the end of the signal for optimal processing. Spectrum analysis, including peak identification and integration, was carried out using the VNMR software.

2.4. Batch reaction setup

The batch reactor setup is shown in Fig. 1. For each reaction, a new 40-ml EPA glass vial with an open cap and a PFTE-silicon septum (Fisher Scientific) was used as the batch reactor. The reactor contained an X-crossed PTFE magnetic stirrer (Fisher Scientific). Initially, 45 mg of TS-1 was loaded into the reactor vial, followed by the addition of the solvent. The vial was then capped, and all other reagents (mesitylene [99.8%, Aldrich] as the internal standard, 1-hexene [99+%, Aldrich], and solvent [99+%, Aldrich]) were added by injection through the septum via syringes fitted with 26-gauge point style 2 needles (Hamilton). The quantities of each component added were determined by weight. The total reaction volume

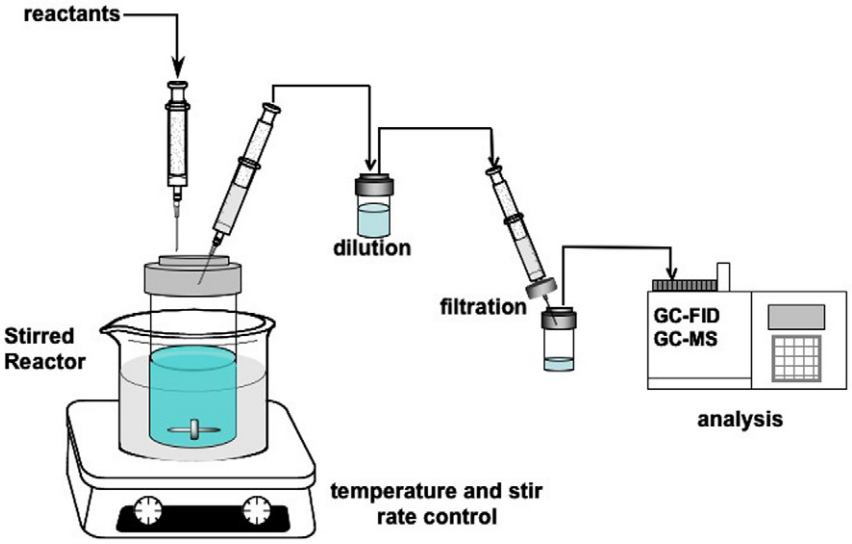

Fig. 1. Batch reactor experimental setup.

was 15 ± 1 ml. The loaded reactor was sonicated for 3 min, then immersed in a 35 °C water bath and allowed to equilibrate for 30 min to the reaction temperature of 35 ± 1 °C. The reaction was started by injection of hydrogen peroxide (50% aq, Aldrich) and DDI water via gas-tight syringes. Samples were taken by extracting 40 µl of reaction liquid through a 50-µl gas-tight syringe, injecting into a silanized autosampler vial (Fisher Scientific) containing 1 ml of chilled solvent, followed immediately by filtration through a 25-mm-diameter, 0.1-µm pore size syringe filter (Fisher Scientific) and then injection into a separate, capped autosampler vial. An additional 1 ml of solvent was pushed through the filter to rinse and capture as much product as possible. The first reaction sample was taken approximately 30 s after the injection of H_2O_2. Subsequent samples were obtained at regular intervals during the reaction. All samples were analyzed by an Agilent 6890+ Plus GC-FID with an HP (5%-phenyl)-methylpolysiloxane column and fitted with an autosampler. A gas-tight 10-ml autosampler syringe was used for the autosampler. It was washed 5 times in solvent before and after extraction from each sample vial. Before a reaction run analysis, calibration samples were prepared and analyzed. To ensure representative area counts, calibration samples were obtained from 15-ml liquid mixtures containing mesitylene, 1,2-epoxyhexane (99.6%, Sigma–Aldrich), 1,2-hexanol, and 1-hexene. Similar to the reaction samples, 40 µl of the liquid calibration mixture was extracted via a syringe and then injected into an autosampler vial containing 1.5 ml of solvent.

2.5. Parameter estimation

Two methods were used to estimate unknown kinetic parameters. The *fmincon* function of Matlab and the MicroSoft Office 2004 Excel Solver function [53,54] were used to minimize the sum of the least squares difference between the observed and predicted initial rates. Initial estimates for the parameters were also varied for each method to sample a larger range of the solution space and seek the global optimum for the solution space more aggressively. Results for the lowest objective function value are reported.

Table 1
Summary of TS-1 characterization results

	TS-1 sample	Technique
Framework structure	MFI	XRD
Framework Ti content	1.3 mol%	XRD, IR, UV–vis
Extra-framework Ti content	None	XRD/ICP, UV–vis
Impurities (Na, K, Fe, Al)	None	ICP
Crystal size	0.2 µm	SEM
Crystal morphology	Cubic and uniform	SEM
Surface Ti content	0.9 mol%	XPS
Surface area	235 m^2/g	BET

3. Results and discussion

3.1. Characterization

The synthesized TS-1 sample was highly crystalline, contained 1.3 mol% Ti in the framework, and contained no extra-framework Ti. The synthesized silicalite samples were highly crystalline and contained no titanium or impurities. Results from the various characterization techniques are summarized in Table 1. The SEM image of TS-1 is shown in Fig. 2, and the DR UV-Vis spectra of TS-1, fresh and regenerated, are shown in Fig. 3. Regenerated catalyst showed the same characteristics as freshly synthesized TS-1; this has been shown to be the case in the literature as well [55]. A more detailed summary of the characterization results is provided in [56].

3.2. 1-Hexene chemisorption versus physisorption

Comparison between 1-hexene adsorption isotherms in TS-1 and silicalite for the methanol system are shown in Fig. 4. There is little difference in the loading between TS-1 and silicalite. Also, the difference is within 0.5 molecules per unit cell, with no discernible trend. This indicates that 1-hexene is not

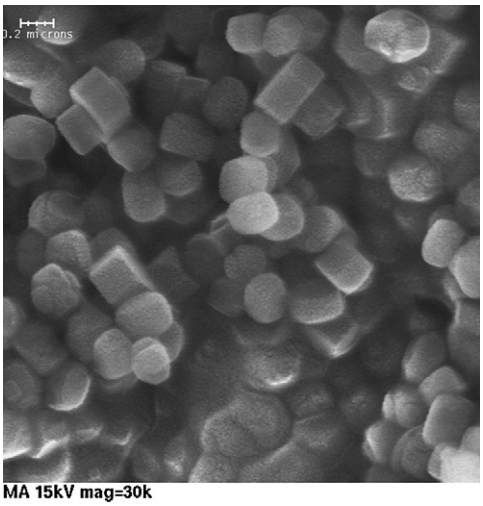

Fig. 2. SEM image of TS-1. Scale bar is 0.2 microns.

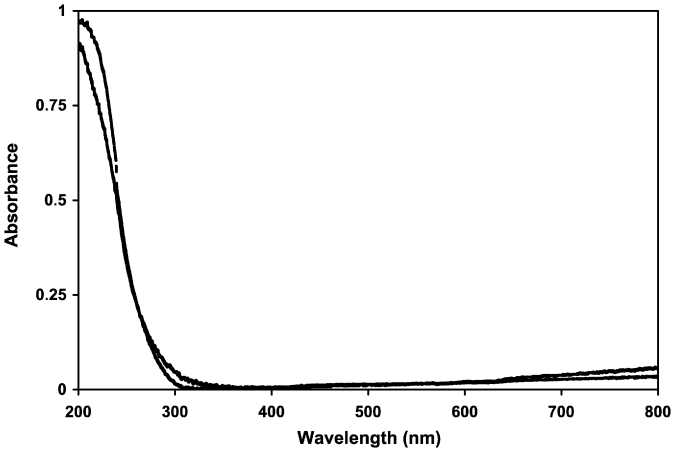

Fig. 3. UV–vis spectrum of TS-1: fresh catalyst before use in any reaction (bottom line at 200 nm) and spent catalyst from reactions which was re-calcined (top line at 200 nm).

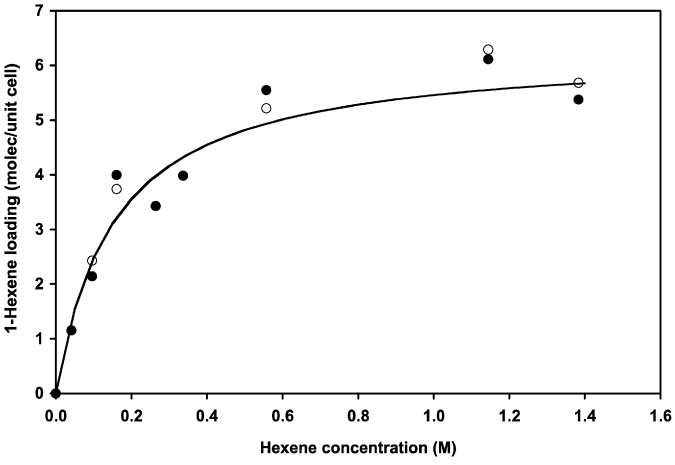

Fig. 4. Adsorption of 1-hexene in silicalite-1 (○) and TS-1 (●) for the methanol system at 295 K. The line corresponds to a Langmuir fit.

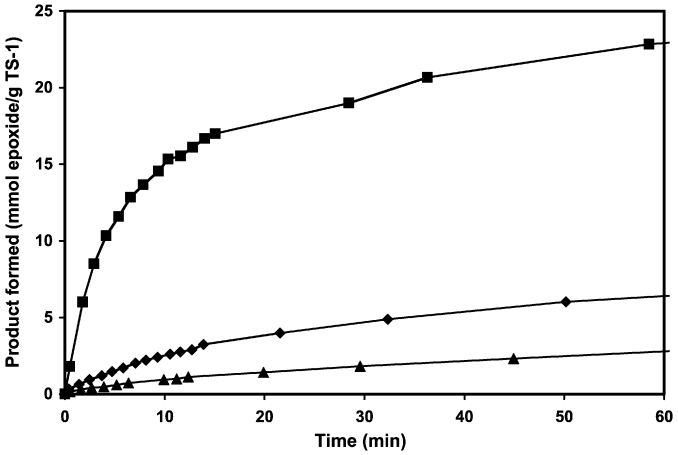

Fig. 5. 1-Hexene epoxidation reaction data for methanol (■), acetonitrile (◆), and acetone (▲) as the solvent with 0.9 M 1-hexene, 1 M H_2O_2, and 4 M H_2O at 308 K.

chemisorbed on the Ti sites, and supports quantum chemical calculation results reported previously [44,57].

3.3. Initial rates and deactivation

Fig. 5 shows examples of the reaction data obtained as a function of time for each solvent system. For the initial rate, the amount of 1,2-epoxyhexane formed was determined in the low-conversion region before one minute. At 60 min, the amounts of product formed have begun to plateau, but the conversion has only reached 8.9% for methanol, 2.8% for acetonitrile, and 1.6% for acetone, indicating that the reactions in TS-1 suffer from deactivation.

3.4. Side products

No side products were detected in the first minute when initial rates were determined. Although formation of 1-methoxyhexan-2-ol, 2-methoxyhexan-1-ol, and 1,2-hexanediol was observed for the methanol system, and 1,2-hexanediol was observed at long reaction times for the acetone and acetonitrile systems, the number of moles of each side product formed was at least two orders of magnitude lower than the amount of 1,2-epoxyhexane formed. This indicates that the TS-1 used in this study was highly selective toward 1,2-epoxyhexane, and side product formation was negligible.

3.5. Concentration dependence

The dependency of the initial rates on the bulk concentrations of 1-hexene, H_2O_2, and water was determined as shown in Figs. 6–8. Keeping the hydrogen peroxide and water concentrations constant at 0.7 and 4 M, respectively, the 1-hexene concentration was varied to determine the reaction order with respect to 1-hexene for each solvent. As shown in Fig. 6, the initial rates were highest in methanol and lowest in acetone. For each solvent, the reaction order decreased to zero as the bulk 1-hexene concentration increased.

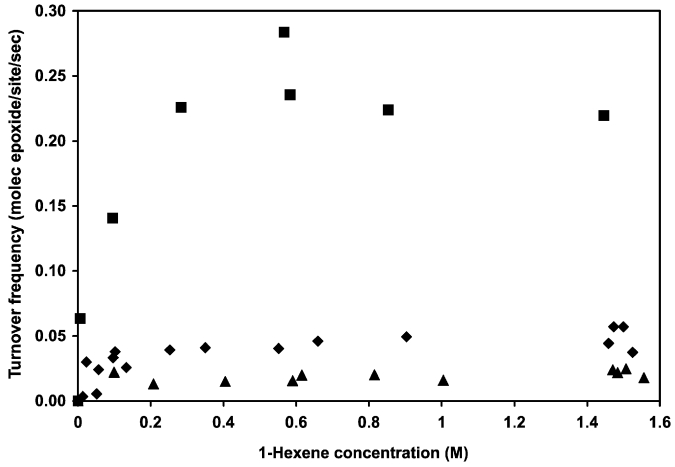

Fig. 6. Initial rate as a function of 1-hexene concentration obtained experimentally for methanol (■), acetonitrile (◆), and acetone (▲) with 0.7 M H_2O_2, 4 M H_2O at 308 K.

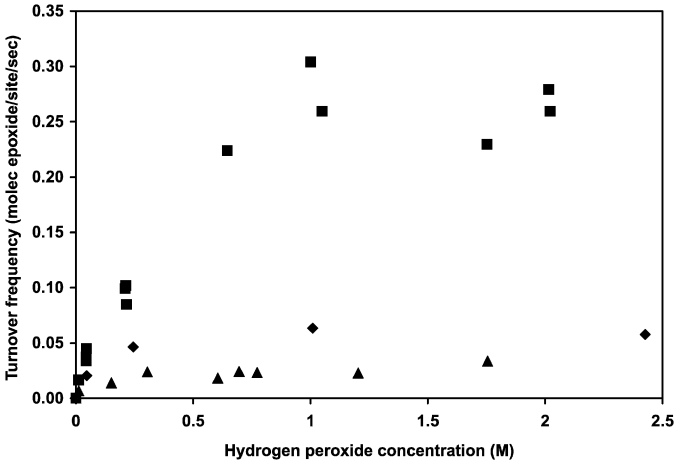

Fig. 7. Initial rate as a function of hydrogen peroxide concentration obtained experimentally for methanol (■), acetonitrile (◆), and acetone (▲) with 0.8 M 1-hexene and 4 M H_2O at 308 K.

A similar dependence of the initial rate on the hydrogen peroxide concentration was observed when the 1-hexene and water concentrations were held constant at 0.8 and 4 M, respectively. Similar to the results when 1-hexene was varied, the highest initial rates were observed for the methanol system, followed by acetonitrile and then acetone, as shown in Fig. 7.

In the case where the 1-hexene and hydrogen peroxide concentrations were constant at values of 0.9 and 0.2 M, respectively, but the water concentration was varied, the initial rates were found to be approximately independent of the bulk water concentration, as depicted in Fig. 8. As in the previous cases, the initial rates were highest in methanol, followed by acetonitrile and acetone.

3.6. Reaction mechanism

Based on the reaction kinetics data, the lack of measurable adsorption of 1-hexene on the active site, and current knowledge of the active site species in the literature, an Eley–Rideal-type reaction mechanism was proposed to capture the reaction

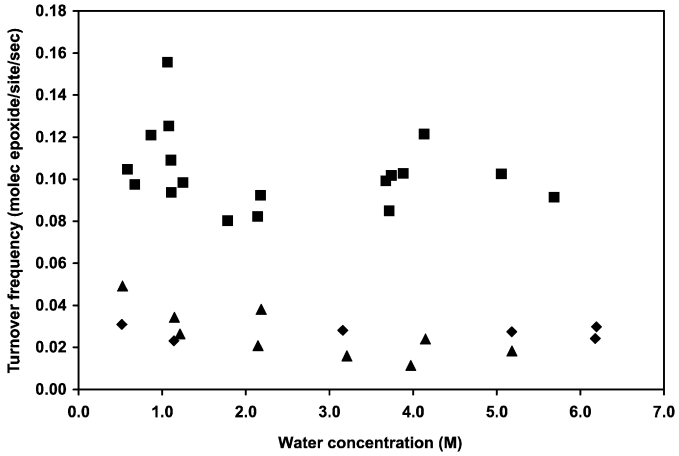

Fig. 8. Initial rate as a function of water concentration obtained experimentally for methanol (■), acetonitrile (◆), and acetone (▲) with 0.9 M 1-hexene and 0.2 M H_2O_2 at 308 K.

kinetics data, as shown in Fig. 9. The titanium site first reacts with a hydrogen peroxide molecule to form the titanium hydroperoxo species, which may or may not be coordinated with a solvent or water molecule. This titanium hydroperoxo species then reacts with a physisorbed 1-hexene molecule to form chemisorbed 1,2-epoxyhexane and water. The 1,2-epoxyhexane is then desorbed, regenerating the titanium active site. The proposed mechanism also takes into account that water may adsorb competitively on the titanium site.

3.7. Reaction rate equation

It has been shown that 1-hexene epoxidation in TS-1 is not diffusion-limited [50]. Thus, assuming that the reaction between the titanium hydroperoxo species and the physisorbed 1-hexene is the rate-limiting step and that all other steps are in quasi-equilibrium, the following reaction rate equation was derived:

$$r = \frac{k_2[*_{\text{total}}](K_1[O][H] - \frac{[W][E]}{K_2K_3})}{1 + K_1[O] + \frac{[E]}{K_3} + \frac{[W]}{K_4}}, \tag{1}$$

where $[O]$, $[H]$, $[W]$, and $[E]$ refer to the intraporous concentrations of hydrogen peroxide, 1-hexene, water, and 1,2-epoxyhexane, respectively; K_i represents the adsorption equilibrium constant for elementary step i that is equal to the ratio of the forward and reverse rate coefficients; and $[*_{\text{total}}]$ refers to the total number of titanium sites. The assumption of 1-hexene addition as the rate-determining step (RDS) is consistent with the theoretical calculations of Panyaburapa et al. [49], whose conclusion was based on energy barriers calculated using ONIOM energies, and our experimental data, as we show below. Wells et al. [47] conducted a rigorous free energy analysis for propylene epoxidation and concluded that formation of the hydroperoxy intermediate is the RDS for a proposed active site of a Ti defect in a full silanol "nest." However, assuming that this step is the RDS for 1-hexene epoxidation would fail to capture the observed dependence of the rate on 1-hexene con-

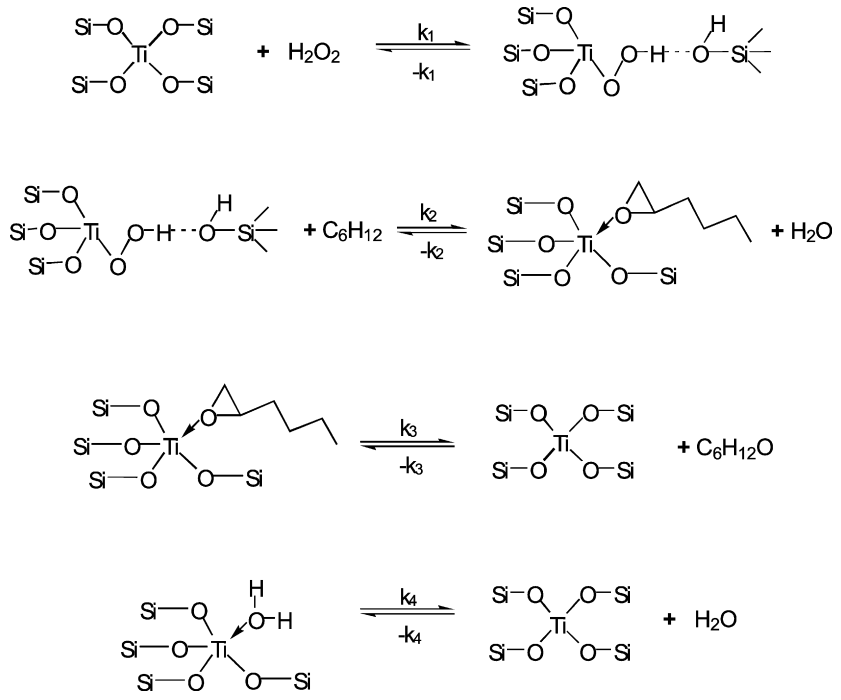

Fig. 9. Proposed reaction mechanism for the liquid-phase epoxidation of 1-hexene in TS-1. All steps are shown as reversible in accord with the principle of microscopic reversibility. However, the rate expression that was compared against the data (Eq. (2)) only included the reaction to form epoxide in the forward direction since only initial rates were measured.

centration. The initial rate, r_0, is obtained from Eq. (1) as

$$r_0 = \frac{k_2[*_{\text{total}}]K_1[O][H]}{1 + K_1[O] + K_4'[W]}, \tag{2}$$

where K_4' is equal to K_4^{-1}. Note that whereas the amount of water produced via reaction is small in the initial rate region, water is present at all times due to the use of aqueous hydrogen peroxide. To express the above reaction rate in terms of experimentally measurable quantities, the adsorption isotherms for each component in TS-1 must be known, because the concentrations on which r_0 depends are intraporous concentrations.

3.8. Adsorption isotherms

Ternary adsorption experiments in TS-1 were carried out in the same concentration range as the reaction experiments to determine the equilibrium relationship between bulk and intraporous 1-hexene concentrations, as shown in Fig. 10 for the three solvent systems. Langmuir-type adsorption behavior was exhibited for the methanol and acetonitrile systems, whereas 1-hexene adsorption followed Henry's law for the acetone system over the concentration range studied. Equation (3) was used to describe the isotherms in all three solvents. The constants q_{sat} and b were fitted using the method of least squares and are listed in Table 2:

$$[H] = q_{\text{sat}}\left(\frac{b[H_{\text{bulk}}]}{1 + b[H_{\text{bulk}}]}\right). \tag{3}$$

Over the same range of 1-hexene concentrations as studied in the reactions, the olefin loading in TS-1 was highest in

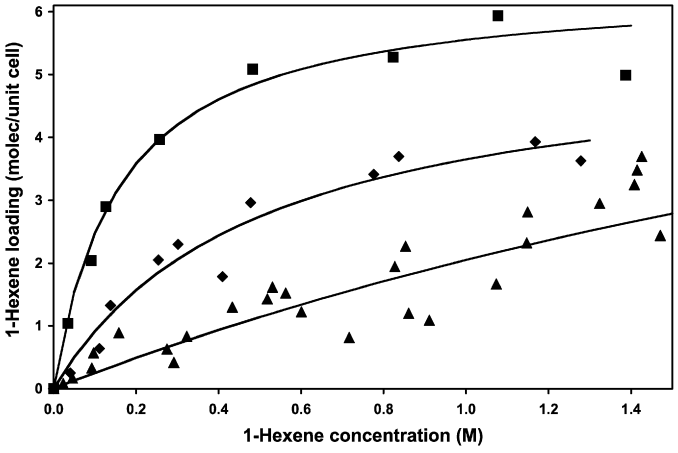

Fig. 10. Ternary adsorption isotherms of 1-hexene in TS-1 with deuterated methanol (■), acetonitrile (◆), and acetone (▲) with 1 M H_2O at 295 K. The lines correspond to Eq. (3).

Table 2
Experimental adsorption isotherm parameters for 1-hexene adsorption in the ternary component system with 1 M H_2O

Solvent system	q_{sat} (molecule/u.c.)	b (L/mol)	$q_{\text{sat}}b$ (dimensionless)
Methanol	6.4	6.3	12.5
Acetonitrile	5.5	2.0	3.4
Acetone[a]	–	–	0.6

[a] The adsorption isotherm for acetone was linear over the entire 1-hexene concentration range investigated. Therefore, only a single parameter, $q_{\text{sat}}b$, was regressed in this case.

Table 3
Adsorption isotherm parameters from GCMC simulations for water adsorption in the ternary component system in silicalite at 308 K [56]

Solvent system	q_{sat} (molecule/u.c.)	b (L/mol)	$q_{sat}b$ (dimensionless)
Methanol[a]	–	–	1.2×10^{-3}
Acetonitrile	19.35	0.411	2.5×10^{0}
Acetone[a,b]	–	–	1.5×10^{-3}

The 1-hexene concentration was fixed at 0.9 M.
[a] The adsorption isotherm for water in methanol and acetone was linear over the entire water concentration range investigated. Therefore, only a single parameter, $q_{sat}b$, was regressed.
[b] Model for acetone was not optimized in the Henry's law region.

methanol, followed by acetonitrile, and then acetone. The order in the Henry's constants ($q_{sat}b$) was also methanol > acetonitrile > acetone, which is in agreement with trends observed in the literature [33].

The solvent order is consistent with trends observed in the reaction kinetics as shown in Figs. 6–8. It is very important to note that TS-1 has a very high internal surface area, so that the reaction occurs mostly within the pore channels. The greater adsorption of 1-hexene in the pores means that more reactant molecules are available to the titanium active sites for reaction when methanol is used compared with acetonitrile, which in turn has a higher number of intraporous 1-hexene molecules than the acetone system.

The adsorption isotherms for water in methanol and acetonitrile solvents were obtained through grand canonical Monte Carlo simulations [56,58]; the parameters are listed in Table 3. In methanol solvent, the intraporous water concentration, $[W]$, is essentially zero; thus, $K_4'[W]$ can be neglected in Eq. (2). Water was adsorbed in significant quantities in acetonitrile solvent. However, the initial rate in acetonitrile (Fig. 8) is independent of the bulk water concentration, and hence the intraporous water concentration. Thus, $K_4'[W]$ must be much less than 1 and is negligible, indicating that K_4' is small in acetonitrile. From the simulations, negligible amounts of water were found to adsorb in acetone solvent, and the initial rate in acetone also is roughly independent of the bulk water concentration, so $K_4'[W]$ is negligible for acetone as well. For all three solvents, either K_4' or $[W]$ (or possibly both for methanol and acetone) is small, and thus the reaction rate is independent of the bulk water concentration.

We could not establish the hydrogen peroxide adsorption behavior experimentally. However, as shown in Fig. 7, the dependence of the initial rate on the bulk hydrogen peroxide concentration is very similar to that observed for the dependence on the 1-hexene concentration, in which case the plateau in the initial rate can be attributed in part to saturation of 1-hexene in the pores. Thus, we can hypothesize that hydrogen peroxide physisorption follows the Langmuir form as well:

$$[O] = q_{H_2O_2} \frac{b_{H_2O_2}[O_{bulk}]}{1 + b_{H_2O_2}[O_{bulk}]}. \tag{4}$$

Whereas the right side of Eq. (2) does not contain $[E]$, the observed concentration of 1,2-epoxyhexane in the bulk, $[E_{bulk}]$, is what is measured, so the rate of formation of E_{bulk} must be related to the rate shown in Eq. (2). Because very small amounts (1×10^{-5}–3×10^{-4} M) of bulk 1,2-epoxyhexane were observed in the initial rate region, its physisorption was assumed to follow Henry's law. Thus, the intraporous concentration of 1,2-epoxyhexane, $[E]$, can be expressed as

$$[E] = K_e[E_{bulk}], \tag{5}$$

where K_e is a dimensionless Henry's constant for 1,2-epoxyhexane. No physisorption parameters for 1,2-epoxyhexane have been reported in the literature. Commercially available 1,2-epoxyhexane contains acetic acid and is not reliable for use in adsorption experiments, because acid-assisted reaction of the 1,2-epoxyhexane with methanol and/or water leads to the formation of ring-opened products, thus leading to the inaccurate accounting of 1,2-epoxyhexane concentrations. Thus, K_e could not be determined independently.

Combining Eqs. (3), (4), and (5) with Eq. (2) results in the following initial rate equation:

$$r_0 = [*_{total}] \frac{k_2}{K_e} \frac{K_1 q_{H_2O_2} b_{H_2O_2}[O_{bulk}] \frac{q_{sat}b[H_{bulk}]}{1+b[H_{bulk}]}}{1 + b_{H_2O_2}(1 + q_{H_2O_2}K_1)[O_{bulk}]}. \tag{6}$$

3.9. Reaction rate equation parameter estimation

Five unknown parameters are present in Eq. (6): k_2, K_e, K_1, $q_{H_2O_2}$, and $b_{H_2O_2}$. None of these parameters can be determined independently, but rather two independent groups of parameters appear—$\alpha = \frac{k_2 K_1 q_{H_2O_2} b_{H_2O_2}}{K_e}$ and $\beta = b_{H_2O_2}(1 + K_1 q_{H_2O_2})$—such that the initial rate is

$$r_0' = \frac{\alpha[O_{bulk}] \frac{q_{sat}b[H_{bulk}]}{1+b[H_{bulk}]}}{1 + \beta[O_{bulk}]}. \tag{7}$$

Two different cases were considered for regressing parameters α and β. The first case constrained both parameters to be the same for all three solvents. The importance of this is that the intrinsic rate coefficient, k_2, and the physisorption and chemisorption of hydrogen peroxide are presumed to be the same in all three solvents, and thus the observed differences in rate are attributed to the differences in physisorption of 1-hexene alone. This is consistent with the hypothesis put forth by Langhendries et al. [33], who attributed the effect of solvent on 1-hexene epoxidation to adsorption effects. The second case allowed α and β to be different for each solvent, for a total of six parameters. A summary of the model parameters and sum of squares values is provided in Table 4, and the agreement of the model for the two different cases is shown by the lines in Fig. 11. Clearly, the agreement of the model with the experimental data improves when the parameters are not constrained to be the same for all three solvents. This indicates that differences in physisorption of 1-hexene without considering the impact of other species (i.e., hydrogen peroxide and 1,2-epoxyhexane) on its adsorption behavior are not sufficient to account for the observed differences in reactivity among the three solvents. This is quantitatively consistent with the general understanding that the performance of Ti-zeolites more broadly cannot be explained solely by adsorption equilibria [8].

Table 4
Parameters and sum of the least squares for each fitting scenario

Case	Description	Number of parameters	Sum of least squares (molecule/site/s)^2	Solvent	α (L uc/mol/s/molecule)	β (L/mol)
1	α and β in Eq. (7) constrained to be equal for all three solvents	2	1.81×10^{-1}		1.49×10^{-1}	3.45
2	α and β in Eq. (7) allowed to be different for each solvent	6	4.36×10^{-2}	Methanol	1.53×10^{-1}	2.31
				Acetonitrile	6.85×10^{-2}	3.56
				Acetone	8.60×10^{-1}	7.27×10^{1}

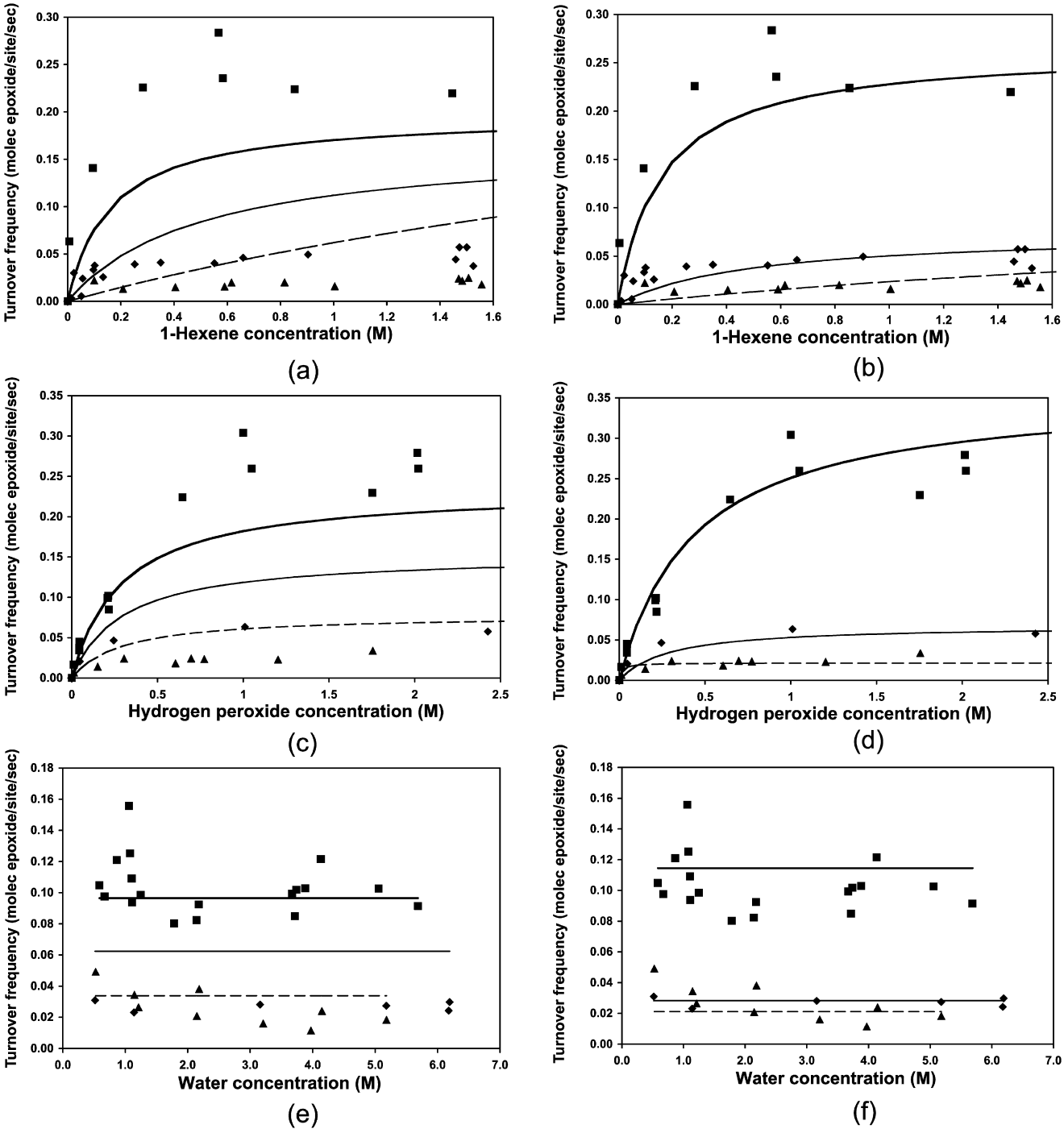

Fig. 11. Comparison of the model fits of the initial rate with the experimental data for the different cases delineated in Table 4: (a) variation of 1-hexene concentration, Case 1; (b) variation of 1-hexene concentration, Case 2; (c) variation of hydrogen peroxide concentration, Case 1; (d) variation of hydrogen peroxide concentration; Case 2; (e) variation of water concentration, Case 1; (f) variation of water concentration, Case 2.

The present experimental results are inconclusive in terms of which of the remaining contributions to the rate (i.e., the intrinsic rate coefficient [k_2], physisorption of 1,2-epoxyhexane [K_e], physisorption of hydrogen peroxide [$q_{H_2O_2}$ and $b_{H_2O_2}$] or chemisorption of hydrogen peroxide [K_1]) dominates, or whether multicomponent adsorption accounting for the effects of H_2O_2 and 1,2-epoxyhexane on 1-hexene physisorption is responsible. However, quantum chemical calculations suggest that chemisorption of H_2O_2 (K_1) is not dependent on the choice of the solvent. Sever and Root [44] showed that the activation barrier and reaction energy for the formation of the titanium hydroperoxo species were essentially the same when coordinated with a methanol or water molecule. It was noted that an aprotic solvent, such as acetone or acetonitrile, results in the coordination of a water molecule around the titanium hydroperoxo species instead, so that water plays the same role in the aprotic solvent system as methanol does in the protic solvent system [44]. Additional experimental or theoretical investigations are needed to further deconvolute the contributions of the intrinsic rate, physisorption of 1,2-epoxyhexane and hydrogen peroxide, and multicomponent adsorption effects.

4. Conclusion

The present study was conducted to gain a more fundamental understanding of the role of the solvent in the reaction kinetics of 1-hexene epoxidation with TS-1 catalyst. More accurate initial reaction rate data than are available in the literature were obtained, and an Eley–Rideal-type mechanism was proposed in which an active titanium hydroperoxo species reacts with physisorbed 1-hexene to form the 1,2-epoxyhexane product. A kinetic model was developed that includes the contributions from adsorption of each species in the reaction. The model was able to capture the data very well when the governing parameters were allowed to vary for the three different solvent systems. It was shown that although the solvent has a significant effect on the adsorption of 1-hexene in TS-1, and hence on the reaction kinetics, these differences alone cannot account for the differences in the observed reaction kinetics. Multicomponent adsorption studies that investigate 1-hexene adsorption in TS-1 in the presence of H_2O_2 and 1,2-epoxyhexane are needed to definitively determine whether the adsorption of 1-hexene is entirely responsible for the differences in reaction rate observed in different solvents.

Acknowledgments

This research was supported by the Chemical Sciences, Geosciences and Biosciences Division, Office of Basic Energy Sciences, Office of Science, US Department of Energy (Grant DE-FG02-03ER15457). The authors gratefully acknowledge the following people at BP (Naperville, IL): Dr. Jim Kaduk for the XRD analysis and Drs. Jaffery Miller and David Sikkenga for their helpful comments and valuable resources. The authors also thank Dr. Joseph Ray (Baxter) for providing helpful suggestions regarding the NMR analysis, and the Analytical Sciences Laboratory and the Keck Facility at Northwestern University for providing access to the XPS and DR UV–vis equipment.

References

[1] M. Taramasso, G. Perego, B. Notari, Preparation of porous crystalline synthetic material comprised of silicon and titanium oxides, US Patent No. 4410501, 1983.
[2] P. Ratnasamy, R. Kumar, Stud. Surf. Sci. Catal. 97 (1995) 367.
[3] M.G. Mantegazza, Petrini, G. Spano, R. Bagatin, F. Rivetti, J. Mol. Catal. A Chem. 146 (1999) 223.
[4] R. Saxton, Top. Catal. 9 (1999) 43.
[5] M.T. Dusi, T. Mallat, A. Baiker, Catal. Rev. 42 (2000) 213.
[6] R.A. Sheldon, I. Arends, A. Dijksman, Catal. Today 57 (2000) 157.
[7] A. Corma, H. Garcia, Chem. Rev. 102 (2002) 3837.
[8] M.G. Clerici, Oil Gas Eur. Mag. 32 (2) (2006) 77.
[9] P. Wu, D. Nuntasri, J. Ruan, Y. Liu, M. He, W. Fan, O. Terasaki, T. Tatsumi, J. Phys. Chem. B 108 (2004) 19126.
[10] D.P. Serrano, G. Calleja, J.A. Botas, F.J. Gutierrez, Sep. Purif. Technol. 54 (2007) 1.
[11] C.-H. Xu, T. Jin, S.H. Jhung, J.-S. Chang, J.-S. Hwang, S.-E. Park, Catal. Today 111 (2006) 366.
[12] I. Arends, R.A. Sheldon, Appl. Catal. A 212 (1–2) (2001) 175.
[13] L. Davies, P. McMorn, D. Bethell, P.C.B. Page, F. King, F.E. Hancock, G.J. Hutchings, Chem. Commun. 18 (2000) 1807.
[14] L. Davies, P. McMorn, D. Bethell, P.C.B. Page, F. King, F.E. Hancock, G.J. Hutchings, Phys. Chem. Chem. Phys. 3 (4) (2001) 632.
[15] L. Davies, P. McMorn, D. Bethell, P.C.B. Page, F. King, F.E. Hancock, G.J. Hutchings, J. Catal. 198 (2) (2001) 319.
[16] J. Jarupatrakorn, T.D. Tilley, J. Am. Chem. Soc. 124 (2002) 8380.
[17] G.N. Vayssilov, Catal. Rev. 39 (3) (1997) 209.
[18] R. Bal, K. Chaudhari, D. Srinivas, S. Sivasanker, P. Ratnasamy, J. Mol. Catal. A Chem. 162 (2000) 199.
[19] D. Gleeson, G. Sankar, C.R.A. Catlow, J.M. Thomas, G. Spano, S. Bordiga, A. Zecchina, C. Lamberti, Phys. Chem. Chem. Phys. 2 (20) (2000) 4812.
[20] A.S. Soult, D.F. Carter, H.D. Schreiber, L.J. van de Burgt, A.E. Stiegman, J. Phys. Chem. B 105 (14) (2001) 2687.
[21] V. Bolis, Langmuir 15 (1999) 5753.
[22] G. Ricchiardi, A. de Man, J. Sauer, Phys. Chem. Chem. Phys. 2 (2000) 2195.
[23] C.A. Hijar, R.M. Jacubinas, J. Eckert, N.J. Henson, P.J. Hay, K.C. Ott, J. Phys. Chem. B 104 (51) (2000) 12157.
[24] P.F. Henry, M.T. Weller, C.C. Wilson, J. Phys. Chem. B 105 (31) (2001) 7452.
[25] T. Atoguchi, S. Yao, J. Mol. Catal. A Chem. 191 (2003) 281.
[26] G. Sastre, A. Corma, Chem. Phys. Lett. 302 (1999) 447.
[27] G.L. Marra, F.A. Artioli, M. Milanesio, C. Lamberti, Microporous Mesoporous Mater. 40 (1–3) (2000) 85.
[28] B. Notari, Adv. Catal. 41 (1996) 253.
[29] J.F. Bengoa, N.G. Gallegos, S.G. Marchetti, A.M. Alvarez, M.V. Cagnoli, A.A. Yeramian, Microporous Mesoporous Mater. 24 (4–6) (1998) 163.
[30] B. Notari, Catal. Today 18 (2) (1993) 163.
[31] C.B. Khouw, C.B. Dartt, J.A. Labinger, M.E. Davis, J. Catal. 149 (1994) 195.
[32] M.G. Clerici, P. Ingallina, J. Catal. 140 (1) (1993) 71.
[33] G. Langhendries, D.E. de Vos, G.V. Baron, P.A. Jacobs, J. Catal. 187 (1999) 453.
[34] D.E. De Vos, J. Denayer, F. van Laar, G.V. Baron, P.A. Jacobs, Top. Catal. 23 (1–4) (2003) 191.
[35] X. Liu, X. Wang, X. Guo, G. Li, Catal. Today 93–95 (2004) 505.
[36] M.G. Clerici, Top. Catal. 15 (2–4) (2001) 257.
[37] G. Bellusi, V. Fattore, Stud. Surf. Sci. Catal. (1991) 79.
[38] P.E. Sinclair, C.R.A. Catlow, Chem. Commun. 19 (1997) 1881.
[39] K. Chaudhari, D. Srinivas, P. Ratnasamy, J. Catal. 203 (2001) 25.
[40] Y.S.S. Wan, J.L.H. Chau, K.L. Yeung, A. Gavriilidis, J. Catal. 223 (2004) 241.

[41] A. Corma, P. Esteve, A. Martinez, Appl. Catal. A 143 (1) (1996) 87.
[42] J.E. Gallot, D.T. On, M.P. Kapoor, S. Kaliaguine, Ind. Eng. Chem. Res. 36 (1997) 3458.
[43] E. Dumitriu, V. Hulea, P. Moreau, Rev. Roum. de Chim. 44 (11–12) (1999) 1073.
[44] R.R. Sever, T.W. Root, J. Phys. Chem. B 107 (17) (2003) 4080.
[45] R.R. Sever, T.W. Root, J. Phys. Chem. B 107 (17) (2003) 4090.
[46] W. Lin, H. Frei, J. Am. Chem. Soc. 124 (2002) 9292.
[47] D.H. Wells Jr., A.M. Joshi, W.N. Delgass, K.T. Thomson, J. Phys. Chem. B 110 (2006) 14627.
[48] E. Spanó, G. Tabacchi, A. Gamba, E. Fois, J. Phys. Chem. B 110 (2006) 21651.
[49] W. Panyaburapa, T. Nanok, J. Limtrakul, J. Phys. Chem. C 111 (2007) 3433.
[50] C.E. Ramachandran, Q. Zhao, A. Zikanova, M. Kocirik, L.J. Broadbelt, R.Q. Snurr, Catal. Commun. 7 (2006) 936.
[51] A. Thangaraj, R. Kumar, S.P. Mirajkar, P. Ratnasamy, J. Catal. 130 (1991) 1.
[52] J.F. Moulder, J. Chastain (Ed.), Handbook of X-Ray Photoelectron Spectroscopy: A Reference Book of Standard Spectra for Identification and Interpretation of XPS Data. Minneapolis, Eden Prairie, 1992.
[53] J. Nocedal, S.J. Wright, Numerical Optimization, Springer-Verlag, New York, 1999.
[54] Frontline Systems, Optimization with Excel Solver, 2005, http://www.solver.com.
[55] M. Clerici, G. Bellusi, U. Romano, J. Catal. 129 (1991) 159.
[56] C.E. Ramachandran, Ph.D. thesis, Solvent effects in the liquid phase epoxidation of 1-hexene with titanium silicalite-1, Northwestern University, Evanston, IL, 2005.
[57] P.E. Sinclair, C.R.A. Catlow, J. Phys. Chem. B 103 (1999) 1084.
[58] C.E. Ramachandran, S. Chempath, L.J. Broadbelt, R.Q. Snurr, Microporous Mesoporous Mater. 90 (1–3) (2006) 293.